Understanding SIDIS data from QCD

J. Osvaldo Gonzalez-Hernandez

University of Turin

Outline

- **Comments on high precision TMD Extractions:**
  - Theoretical limitations
  - Data precision

- **Sivers function in Generalized Parton Picture (new COMPASS analysis of Sivers asymmetry)**

$\boxed{\text{Sivers}}$ asymmetry in SIDIS

$$A_{UT}^{\sin(\phi_h-\phi_S)} = 2\,\frac{\int d\phi_S d\phi_h \left[d\sigma^\uparrow - d\sigma^\downarrow\right] \sin(\phi_h-\phi_S)}{\int d\phi_S d\phi_h \left[d\sigma^\uparrow + d\sigma^\downarrow\right]} = \frac{F_{UT}^{\sin(\phi_h-\phi_S)}}{F_{UU}}$$

Anselmino, et al. Phys.Rev. D71 (2005) 074006

Anselmino, et al. Phys.Rev. D72 (2005) 094007 (Generalized Parton Picture)

Anselmino, et al. Eur.Phys.J. A39 (2009) 89-100

Anselmino, et al. JHEP 1704 (2017) 046 (sign change)

Aybat, et al. Phys.Rev. D86 (2012) 014028 (Theoretical framework/evolution)

Anselmino, et al. Phys.Rev. D86 (2012) 014028 (discussions on pheno/evolution)

Echevarria, et al. Phys.Rev. D89 (2014) 074013 (extraction with evolution SCET)

$\boxed{\text{Sivers}}$ asymmetry in SIDIS

$$A_{UT}^{\sin(\phi_h-\phi_S)} = 2\,\frac{\int d\phi_S d\phi_h \left[d\sigma^{\uparrow} - d\sigma^{\downarrow}\right] \sin(\phi_h-\phi_S)}{\int d\phi_S d\phi_h \left[d\sigma^{\uparrow} + d\sigma^{\downarrow}\right]} = \frac{F_{UT}^{\sin(\phi_h-\phi_S)}}{F_{UU}}$$

- **New COMPASS analysis: Q^2 binning of azimuthal asymmetries.**

Phys.Lett. B770 (2017) 138-145

- **Results on new phenomenological analysis by Torino-Cagliari collaboration:**

M. Boglione, U. D'Alesio, C. Flore, JOGH

JHEP 1807 (2018) 148

$\boxed{\text{Sivers}}$ asymmetry in SIDIS

$$A_{UT}^{\sin(\phi_h-\phi_S)} = 2\,\frac{\int d\phi_S d\phi_h\,[d\sigma^{\uparrow}-d\sigma^{\downarrow}]\sin(\phi_h-\phi_S)}{\int d\phi_S d\phi_h\,[d\sigma^{\uparrow}+d\sigma^{\downarrow}]} = \frac{F_{UT}^{\sin(\phi_h-\phi_S)}}{F_{UU}}$$

Generalized Parton Picture (no evolution)

$$\boxed{\Delta^N f_{q/p^{\uparrow}}(x,k_{\perp})} = 4N_q x^{\alpha_q}(1-x)^{\beta_q}\,\frac{M_p}{\langle k_{\perp}^2\rangle_S}\,k_{\perp}\,\frac{e^{-k_{\perp}^2/\langle k_{\perp}^2\rangle_S}}{\pi\langle k_{\perp}^2\rangle_S}$$

Sivers asymmetry in SIDIS

$$A_{UT}^{\sin(\phi_h-\phi_S)} = 2\,\frac{\int d\phi_S d\phi_h\,[d\sigma^\uparrow - d\sigma^\downarrow]\sin(\phi_h-\phi_S)}{\int d\phi_S d\phi_h\,[d\sigma^\uparrow + d\sigma^\downarrow]} = \frac{F_{UT}^{\sin(\phi_h-\phi_S)}}{F_{UU}}$$

Generalized Parton Picture (no evolution)

$$\boxed{\Delta^N f_{q/p^\uparrow}(x,k_\perp)} = 4N_q x^{\alpha_q}(1-x)^{\beta_q}\,\frac{M_p}{\langle k_\perp^2\rangle_S}\,k_\perp\,\frac{e^{-k_\perp^2/\langle k_\perp^2\rangle_S}}{\pi\langle k_\perp^2\rangle_S}$$

TMD evolution (CSS)

$$\boxed{\tilde{F}_{1T}^{\prime\perp f}(x,b_T;\mu,\zeta_F)} = \boxed{\tilde{F}_{1T}^{\prime\perp f}(x,b_T;\mu_0,Q_0^2)}\exp\left\{\ln\frac{\sqrt{\zeta_F}}{Q_0}\tilde{K}(b_*;\mu_b) + \int_{\mu_0}^{\mu}\frac{d\mu'}{\mu'}\left[\gamma_F(g(\mu');1) - \ln\frac{\sqrt{\zeta_F}}{\mu'}\gamma_K(g(\mu'))\right] + \int_{\mu_0}^{\mu_b}\frac{d\mu'}{\mu'}\ln\frac{\sqrt{\zeta_F}}{Q_0}\gamma_K(g(\mu')) - g_K(b_T)\ln\frac{\sqrt{\zeta_F}}{Q_0}\right\}.$$

see Aybat, et al. Phys.Rev. D86 (2012) 014028

Sivers asymmetry in SIDIS

$$A_{UT}^{\sin(\phi_h-\phi_S)} = 2\,\frac{\int d\phi_S d\phi_h \left[d\sigma^{\uparrow} - d\sigma^{\downarrow}\right]\sin(\phi_h-\phi_S)}{\int d\phi_S d\phi_h \left[d\sigma^{\uparrow} + d\sigma^{\downarrow}\right]} = \frac{F_{UT}^{\sin(\phi_h-\phi_S)}}{F_{UU}}$$

Generalized Parton Picture (no evolution)

$$\Delta^N f_{q/p^{\uparrow}}(x,k_\perp) = 4N_q x^{\alpha_q}(1-x)^{\beta_q}\,\frac{M_p}{\langle k_\perp^2\rangle_S}\,k_\perp\,\frac{e^{-k_\perp^2/\langle k_\perp^2\rangle_S}}{\pi\langle k_\perp^2\rangle_S}$$

No constraint from collinear PDF

Gaussian ansatz

Sivers asymmetry in SIDIS

$$A_{UT}^{\sin(\phi_h-\phi_S)} = 2\,\frac{\int d\phi_S d\phi_h\,[d\sigma^\uparrow - d\sigma^\downarrow]\sin(\phi_h-\phi_S)}{\int d\phi_S d\phi_h\,[d\sigma^\uparrow + d\sigma^\downarrow]} = \frac{F_{UT}^{\sin(\phi_h-\phi_S)}}{F_{UU}}$$

$$F_{UT}^{\sin(\phi_h-\phi_S)} \sim \boxed{\Delta^N f_{q/p^\uparrow}(x,k_\perp,Q^2)} \otimes \boxed{D(z,p_\perp,Q^2)}$$

$$F_{UU} \sim \boxed{F(x,k_\perp,Q^2) \otimes D(z,p_\perp,Q^2)}$$

Using results from Anselmino, et al. JHEP 04, 005 (2014),1312.6261

Combined fit of HERMES COMPASS (reanalysis) and Jlab data (excluding K⁻).

$$\Delta^N f_{q/p^\uparrow}(x,k_\perp) = 4N_q x^{\alpha_q}(1-x)^{\beta_q}\,\frac{M_p}{\langle k_\perp^2\rangle_S}\,k_\perp\,\frac{e^{-k_\perp^2/\langle k_\perp^2\rangle_S}}{\pi\langle k_\perp^2\rangle_S}$$

n. of data points = 220		
One flavour fits (3 parameters)		
	$\chi^2_{\rm tot}$	$\chi^2_{\rm dof}$
u	408	1.88
d	914	4.21
Two flavour fits (5 parameters)		
	$\chi^2_{\rm tot}$	$\chi^2_{\rm dof}$
$u, \bar{u}$	266	1.24
$u, \bar{d}$	228	1.06
$\boldsymbol{u, d}$	**213**	0.99

$$\alpha = 0$$

What flavor information can we extract ?

Reference fit

$$\Delta^N f_{q/p^\uparrow}(x,k_\perp) = 4N_q x^{\alpha_q}(1-x)^{\beta_q} \frac{M_p}{\langle k_\perp^2\rangle_S} k_\perp \frac{e^{-k_\perp^2/\langle k_\perp^2\rangle_S}}{\pi\langle k_\perp^2\rangle_S} \qquad \alpha = 0$$

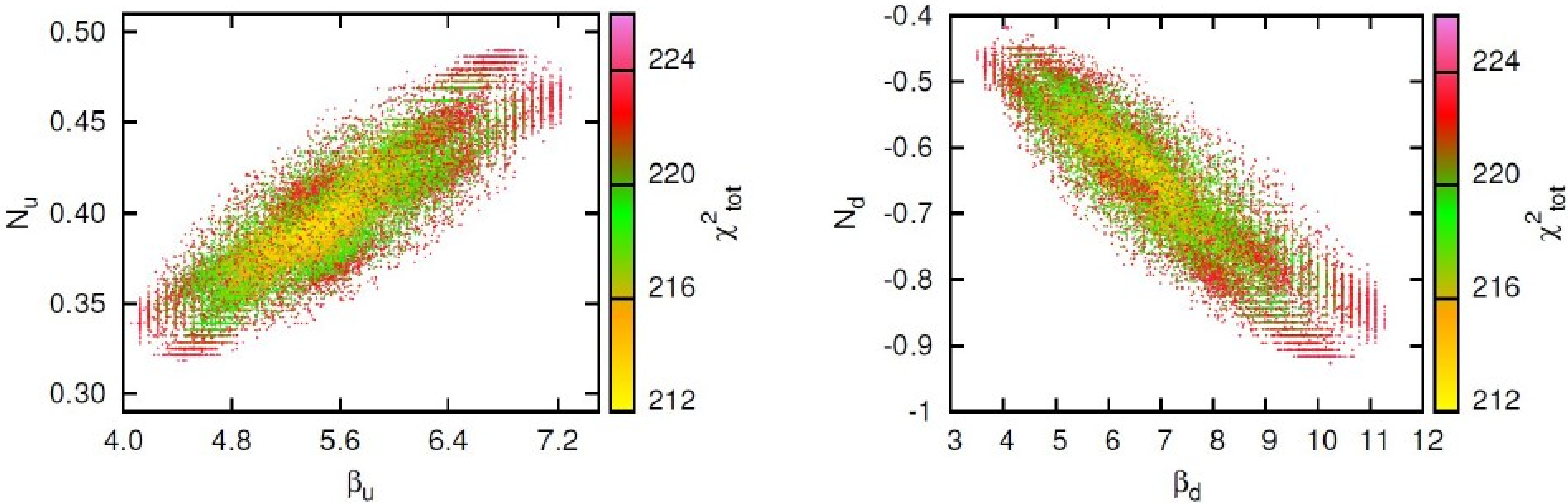

Reference fit - no evolution		
$\chi^2_{\rm tot} = 212.8$	n. of points $= 220$	
$\chi^2_{\rm dof} = 0.99$	n. of free parameters $= 5$	
$\Delta\chi^2 = 11.3$		
HERMES	$\langle k_\perp^2\rangle = 0.57$ GeV^2	$\langle p_\perp^2\rangle = 0.12$ GeV^2
COMPASS	$\langle k_\perp^2\rangle = 0.60$ GeV^2	$\langle p_\perp^2\rangle = 0.20$ GeV^2
$N_u = 0.40 \pm 0.09$	$\beta_u = 5.43 \pm 1.59$	
$N_d = -0.63 \pm 0.23$	$\beta_d = 6.45 \pm 3.64$	
$\langle k_\perp^2\rangle_S = 0.30 \pm 0.15$ GeV^2		

$$\Delta^N f_{q/p^\uparrow}(x,k_\perp) = 4N_q x^{\alpha_q}(1-x)^{\beta_q}\,\frac{M_p}{\langle k_\perp^2\rangle_S}\,k_\perp\,\frac{e^{-k_\perp^2/\langle k_\perp^2\rangle_S}}{\pi\langle k_\perp^2\rangle_S}$$

Varying α

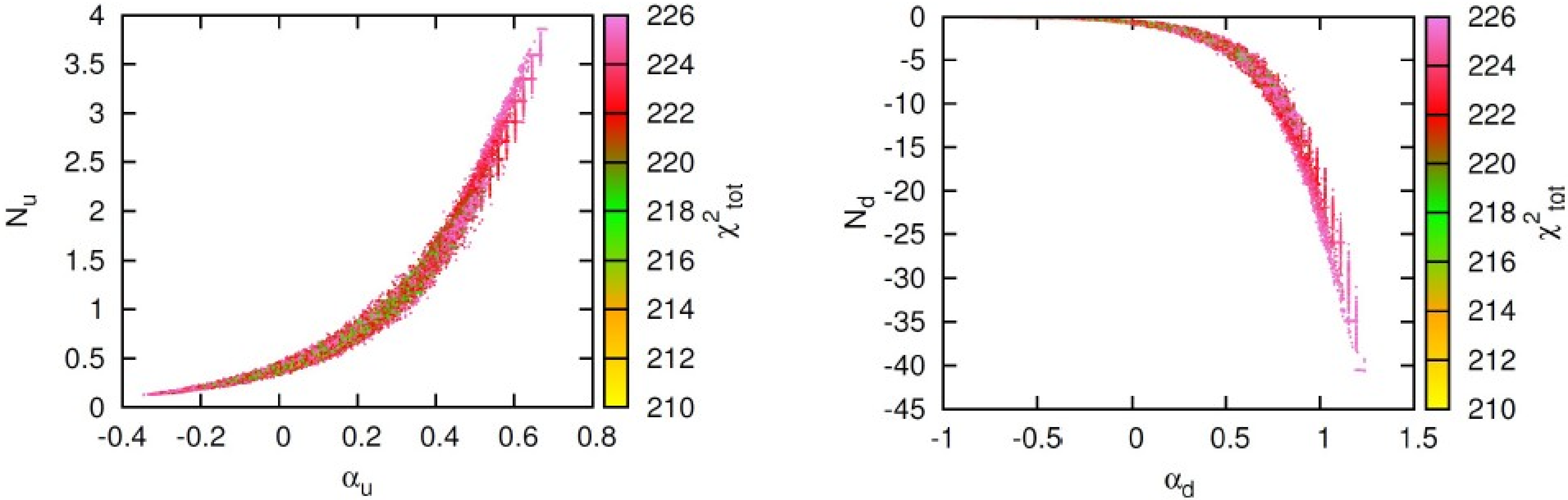

α fit - no evolution		
$\chi^2_{\rm tot} = 211.5$	n. of points = 220	
$\chi^2_{\rm dof} = 0.99$	n. of free parameters = 7	
$\Delta\chi^2 = 14.3$		
HERMES $\langle k_\perp^2\rangle = 0.57$ GeV^2	$\langle p_\perp^2\rangle = 0.12$ GeV^2	
COMPASS $\langle k_\perp^2\rangle = 0.60$ GeV^2	$\langle p_\perp^2\rangle = 0.20$ GeV^2	
$N_u = 0.40 \pm 0.09$	$\beta_u = 5.93 \pm 3.86$	$\alpha_u = 0.073 \pm 0.46$
$N_d = -0.63 \pm 0.23$	$\beta_d = 5.71 \pm 7.43$	$\alpha_d = -0.075 \pm 0.83$
$\langle k_\perp^2\rangle_S = 0.30 \pm 0.15$ GeV^2		

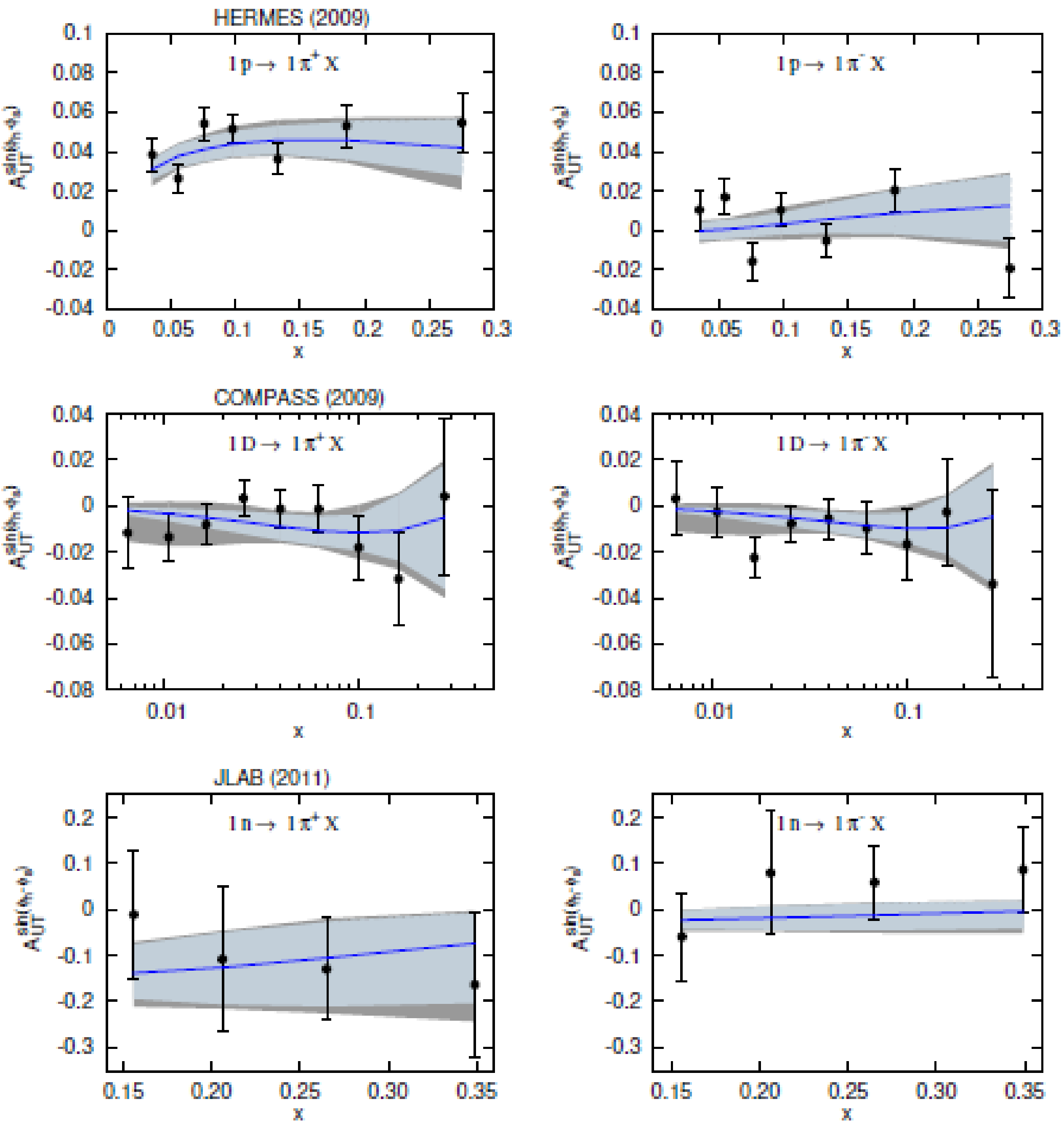

HERMES (2009)
COMPASS (2009)
JLAB (2011)

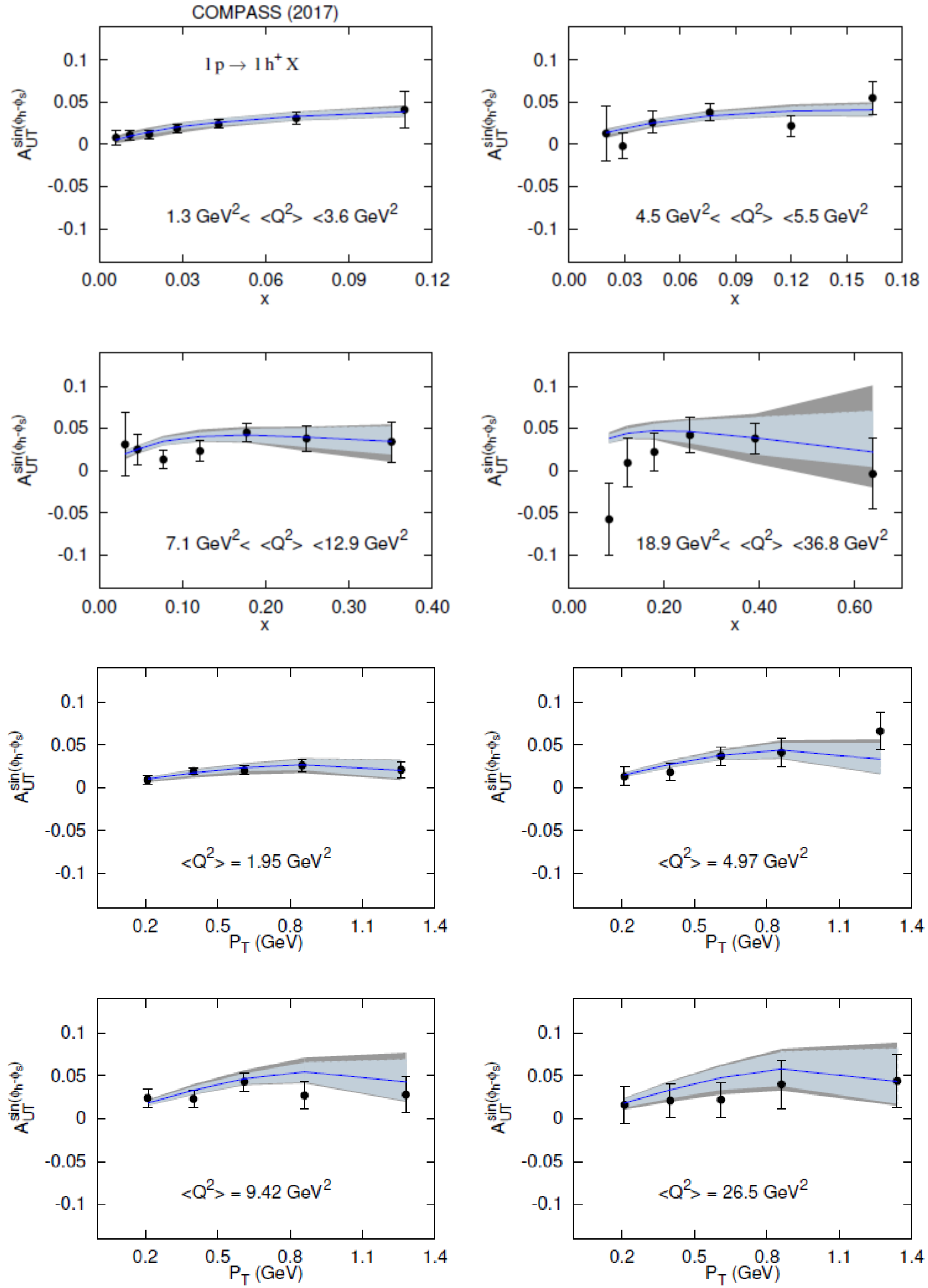
COMPASS (2017)
l p → l h⁺ X
1.3 GeV² < <Q²> <3.6 GeV²
4.5 GeV² < <Q²> <5.5 GeV²
7.1 GeV² < <Q²> <12.9 GeV²
18.9 GeV² < <Q²> <36.8 GeV²
<Q²> = 1.95 GeV²
<Q²> = 4.97 GeV²
<Q²> = 9.42 GeV²
<Q²> = 26.5 GeV²
x
P_T (GeV)
A_UT^sin(φh-φs)

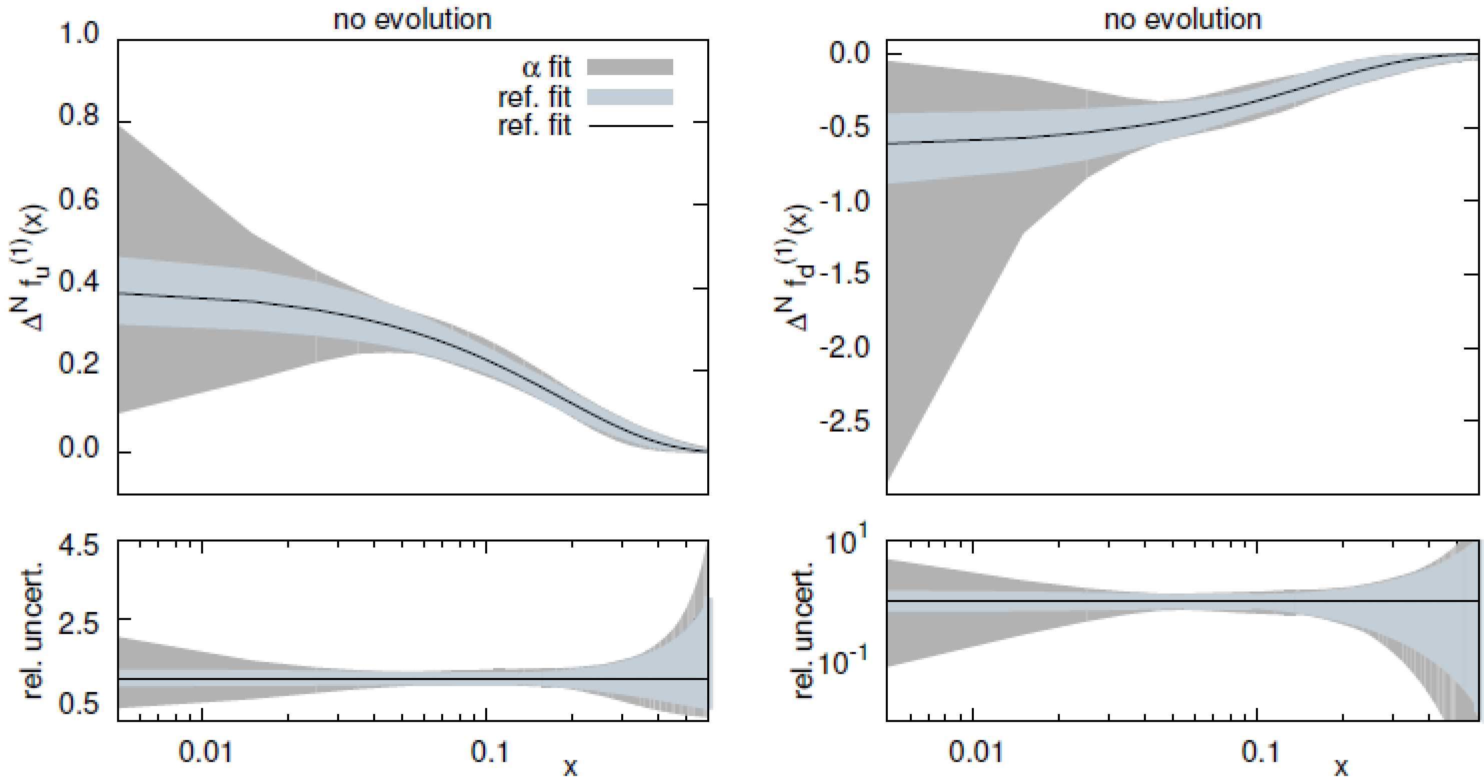

First moment

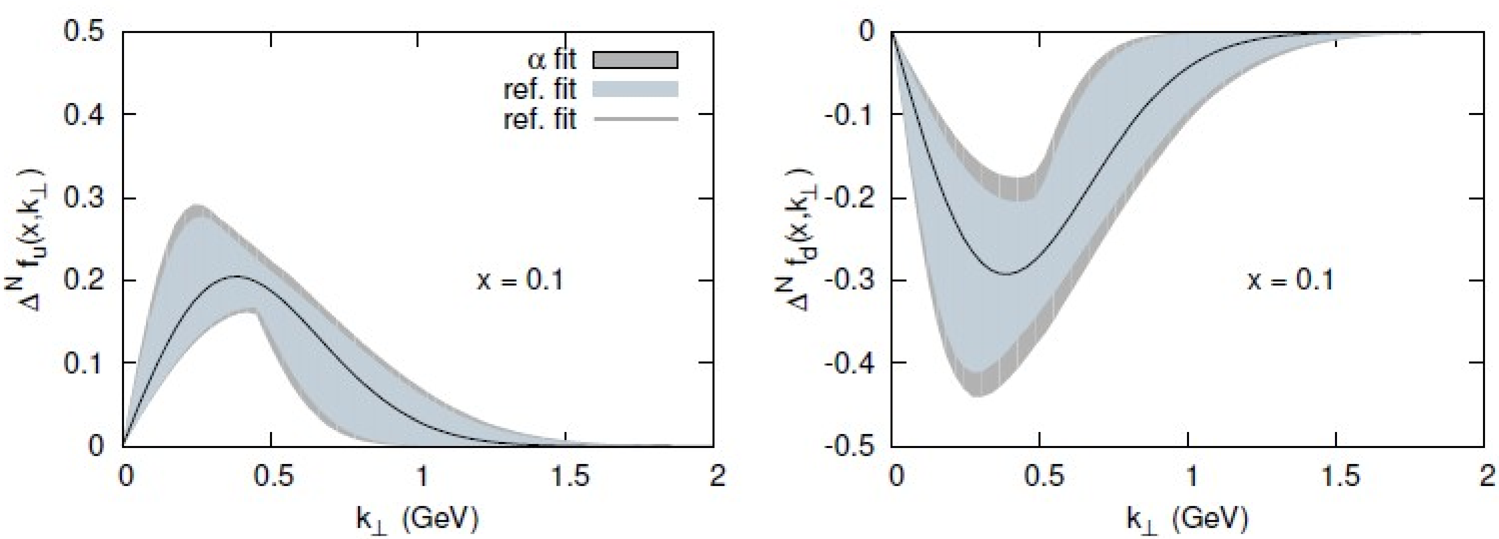

Sivers TMD at fixed value of x

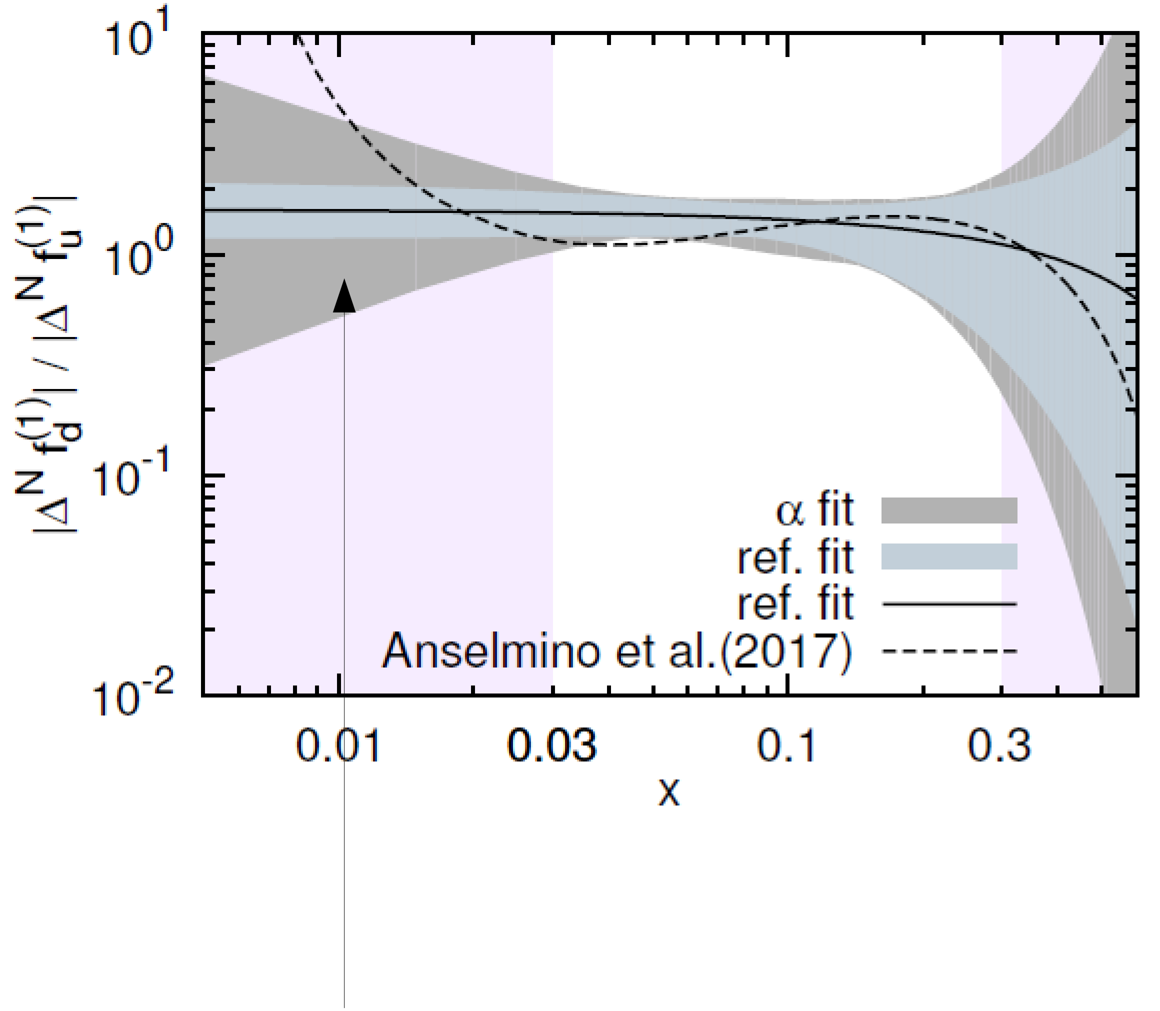

Better assessment of errors at low-x using alpha

Signals of scale dependence (first moment)

$$\frac{\partial T_{q,F}(x,x,\mu)}{\partial \ln \mu^2} = \frac{\alpha_s}{2\pi}\int_x^1 \frac{d\xi}{\xi}\Big\{ P_{qq}(z)\, T_{q,F}(\xi,\xi,\mu)$$
$$+\frac{N_c}{2}\left[\frac{1+z^2}{1-z}\left(\cancel{T_{q,F}(\xi,x,\mu)} - T_{q,F}(\xi,\xi,\mu)\right) + \cancel{z\,T_{q,F}(\xi,x,\mu)} + \cancel{T_{\Delta q,F}(x,\xi,\mu)}\right]$$
$$-N_c\,\delta(1-z)\,T_{q,F}(x,x,\mu) + \frac{1}{2N_c}\left[\cancel{(1-2z)T_{q,F}(x,x-\xi,\mu)} + \cancel{T_{\Delta q,F}(x,x-\xi,\mu)}\right]\Big\}$$

J.B. Kang and J.W. Qiu, Phys. Rev. D 79 (2009) 016003

W. Vogelsang and F. Yuan, Phys. Rev. D 79 (2009) 094010

V.M. Braun, A.N. Manashov, B. Pirnay, Phys. Rev. D 80 (2009) 114002

Z.B Kang and J.W. Qiu, Phys. Lett. B713 (2012) 273-276

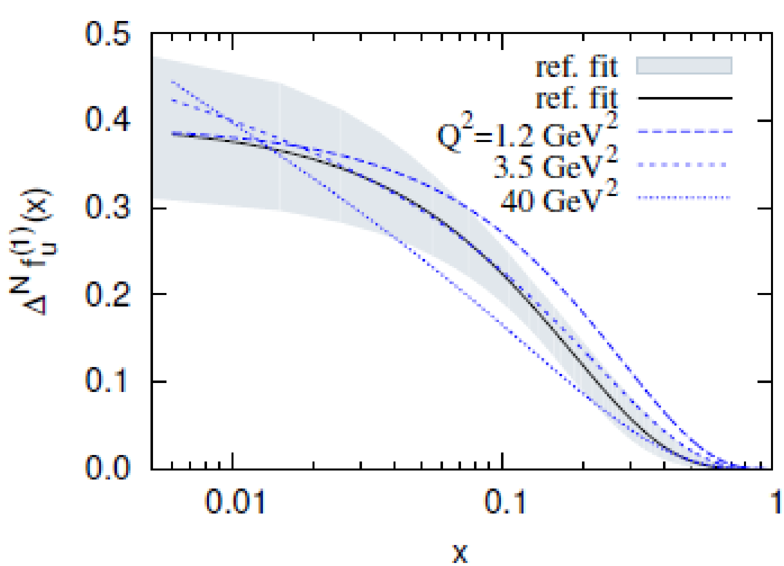

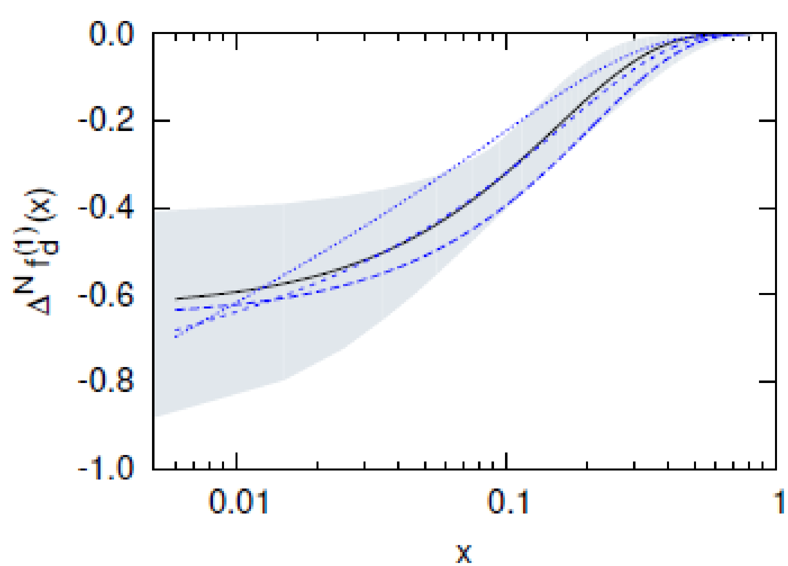

Signals of scale dependence

$$\langle k_\perp^2 \rangle_S = g_1 + g_2 \ln \frac{Q^2}{Q_0^2}$$

g2 here to "mimic" TMD evolution

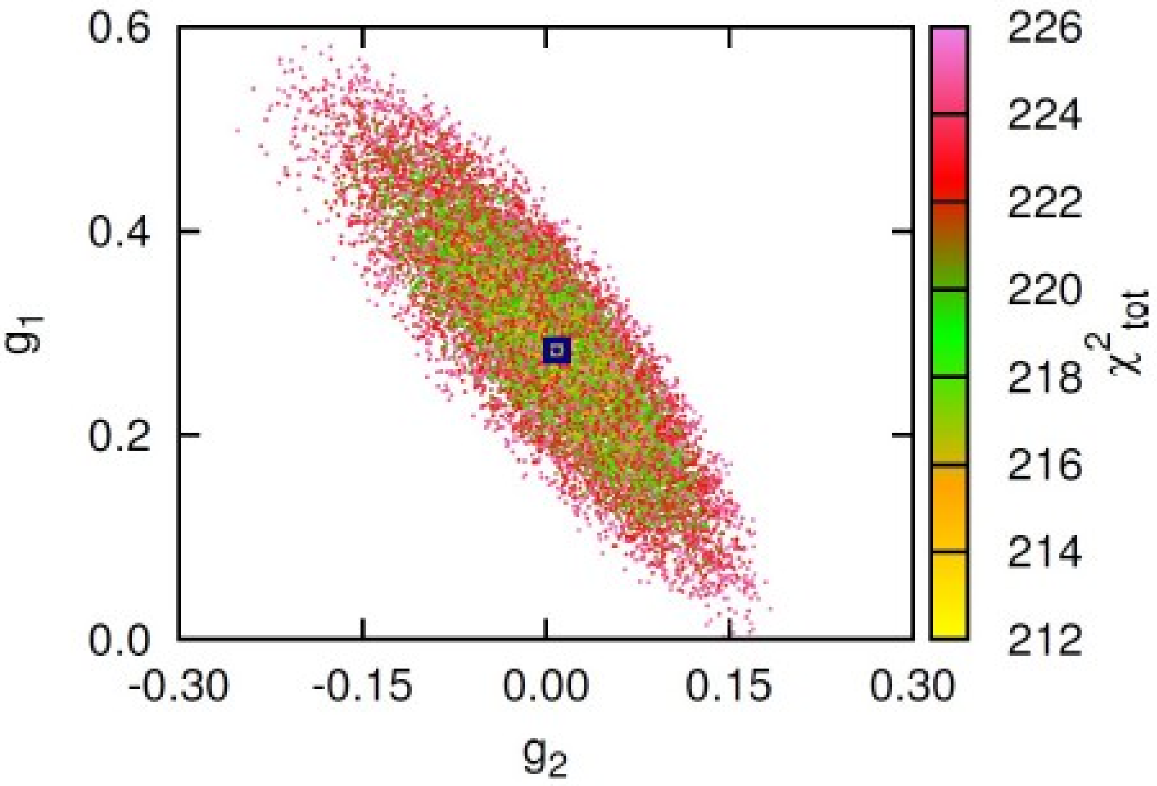

Sivers asymmetry in SIDIS

$$A_{UT}^{\sin(\phi_h-\phi_S)} = 2\,\frac{\int d\phi_S d\phi_h\,[d\sigma^\uparrow - d\sigma^\downarrow]\sin(\phi_h-\phi_S)}{\int d\phi_S d\phi_h\,[d\sigma^\uparrow + d\sigma^\downarrow]} = \frac{F_{UT}^{\sin(\phi_h-\phi_S)}}{F_{UU}}$$

$$F_{UT}^{\sin(\phi_h-\phi_S)} \sim \boxed{\Delta^N f_{q/p^\uparrow}(x, k_\perp, Q^2)} \otimes \boxed{D(z, p_\perp, Q^2)}$$

$$F_{UU} \sim \boxed{F(x, k_\perp, Q^2) \;\otimes\; D(z, p_\perp, Q^2)}$$

Studies on asymmetries strongly depend on our Knowledge of the unpolarized TMDs.

Different assumptions about the unpolarized functions Have dramatic effects on other extractions

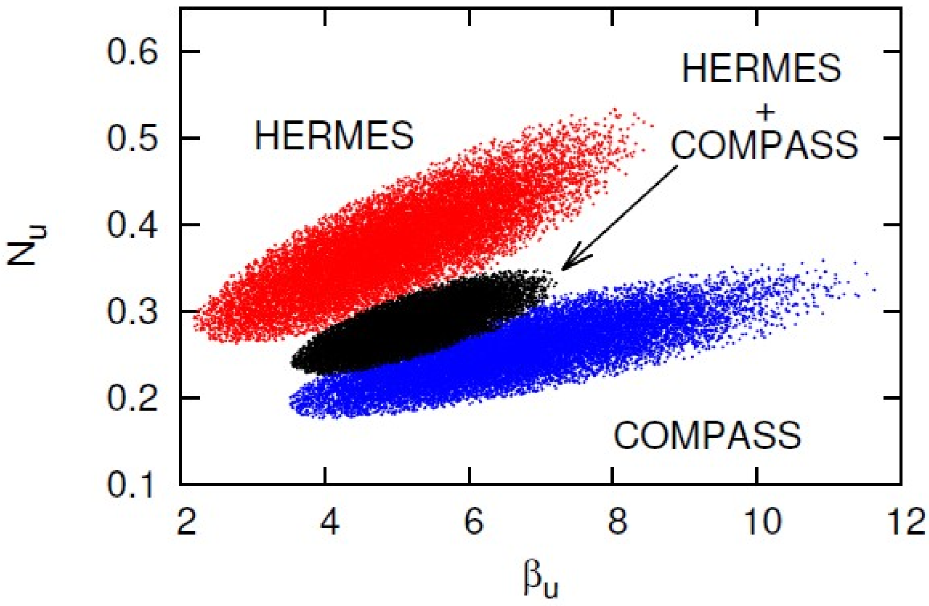

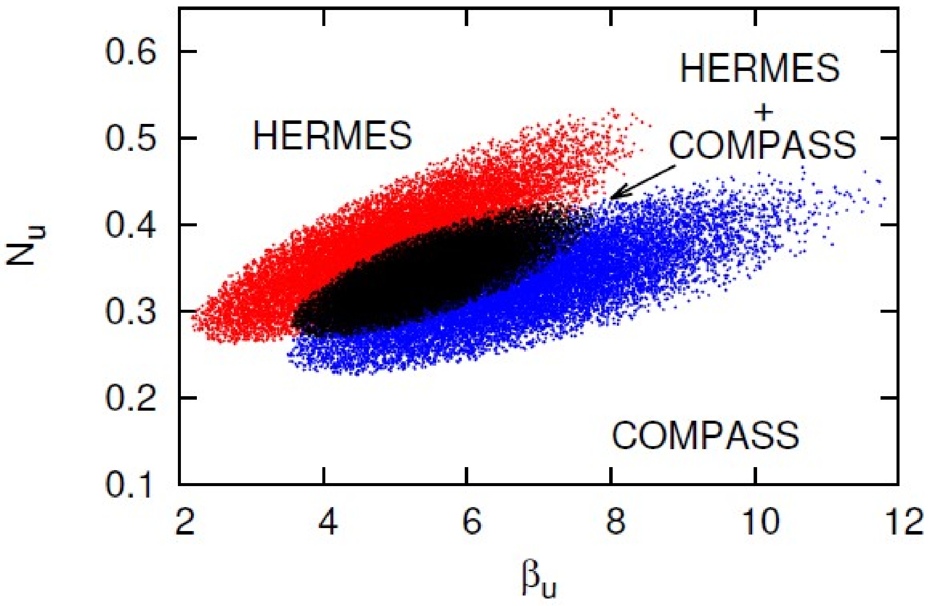

Studies on asymmetries strongly depend on our Knowledge of the unpolarized TMDs.

To proceed to a high precision stage

we first need reliable extractions for unpolarized functions.

The more constraints from first principles the better.

Ultimately, we want to extract TMDs (in all their glory)

Fourier Transform of:

$$\tilde{F}_j(x, b_T, Q, \zeta_F) = \left(\frac{\sqrt{\zeta_F}}{\mu_b}\right)^{\tilde{K}(b_*,\mu_b)} \sum_j \int_x^1 \frac{d\hat{x}}{\hat{x}} \tilde{C}_{ji}^{in}(x/\hat{x}, b_*, \mu_b, \mu_b^2) f_i(\hat{x}, \mu_b)$$
$$\times \exp\left\{\int_{\mu_b}^{Q} \frac{d\mu}{\mu}\left(\gamma_F(\mu;1) - \ln\left(\frac{\sqrt{\zeta_F}}{\mu}\right)\gamma_K(\mu)\right)\right\}$$
$$\times \exp\left\{-g_P(x, b_T) - g_K(b_T)\ln\left(\frac{\sqrt{\zeta_F}}{\sqrt{\zeta_{F0}}}\right)\right\},$$

Unpolarized TMD PDF

$$\tilde{D}_j(z, b_T, Q, \zeta_D) = \left(\frac{\sqrt{\zeta_D}}{\mu_b}\right)^{\tilde{K}(b_*,\mu_b)} \sum_k \int_z^1 \frac{d\hat{z}}{\hat{z}^3} \tilde{C}_{kj}^{out}(z/\hat{z}, b_*, \mu_b, \mu_b^2) D_j(\hat{z}, \mu_b)$$
$$\times \exp\left\{\int_{\mu_b}^{Q} \frac{d\mu}{\mu}\left(\gamma_D(\mu;1) - \ln\left(\frac{\sqrt{\zeta_D}}{\mu}\right)\gamma_K(\mu)\right)\right\}$$
$$\times \exp\left\{-g_H(z, b_T) - g_K(b_T)\ln\left(\frac{\sqrt{\zeta_D}}{\sqrt{\zeta_{D0}}}\right)\right\}.$$

Unpolarized TMD FF

Drell Yan

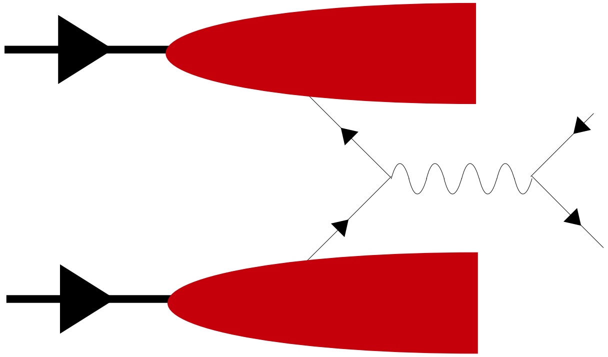

High precision phenomenology:

LO, NLO, NNLO analysis
Eur.Phys.J. C78 (2018) no.2, 89
Ignazio Scimemi, Alexey Vladimirov

Still Some trouble at low energies

Global Fits? First attempts

Drell Yan

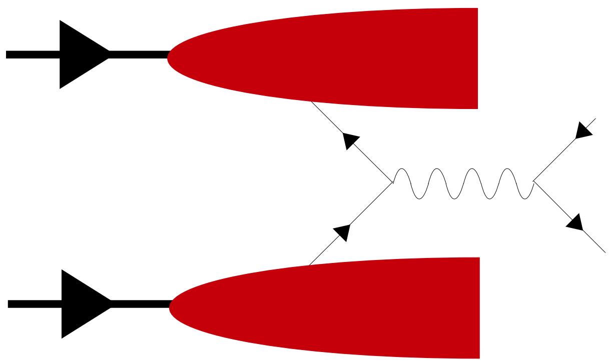

LO analysis
A. Bacchetta, F. Delcarro,
C. Pisano, M. Radici , A. Signori
JHEP 1706 (2017) 081

PDFs

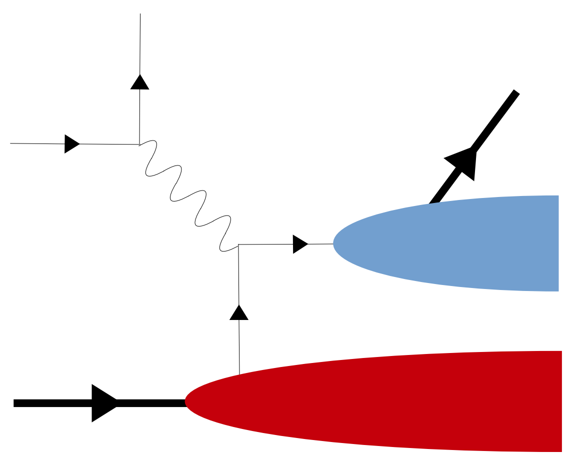

Fragmentation
Functions

SIDIS

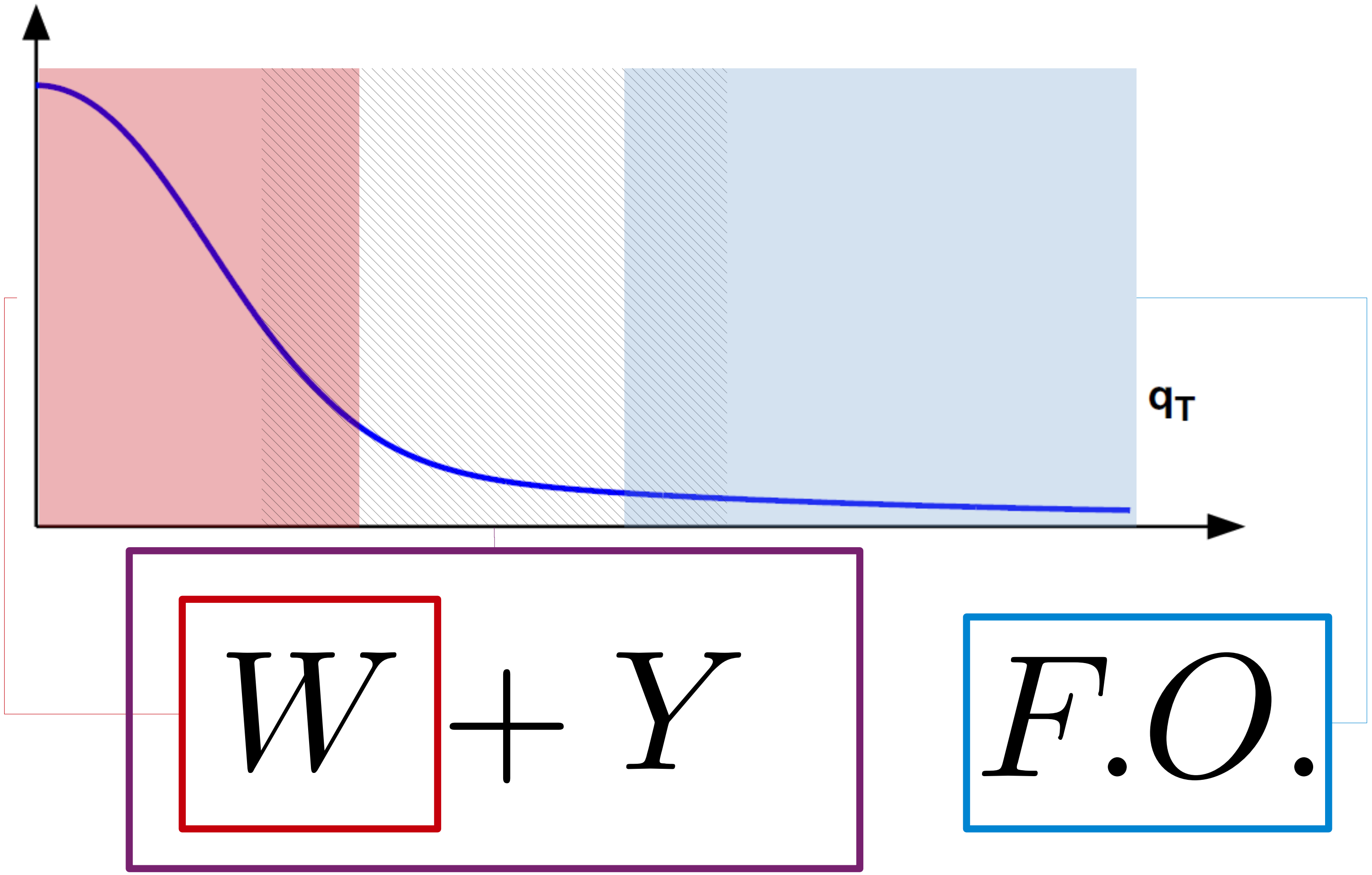

SIDIS variables: $Q^2, \; x_{Bj}, \; z_h, \; P_T$

Often useful to consider: $q_T = P_T / z_h, \;\; y_h = \dfrac{1}{2} \log \left(\dfrac{P_h^+}{P_h^-} \right)$

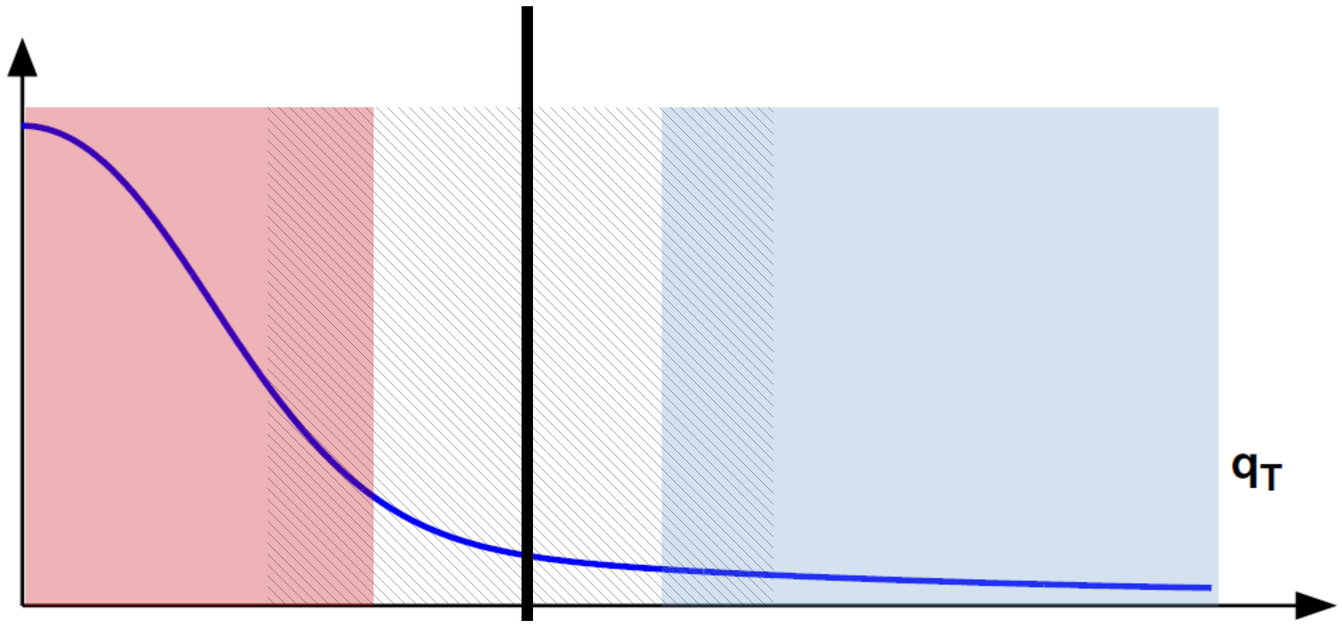

$q_T \sim Q$

Matching region

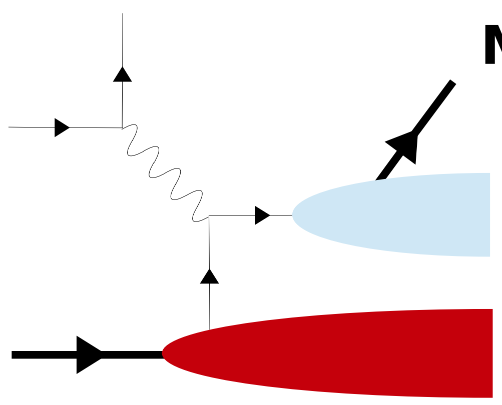

Non-perturbative
Transverse Momentum

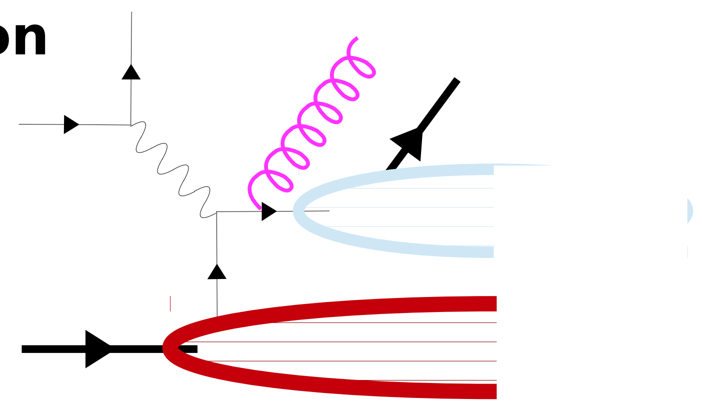

Hard gluon radiation

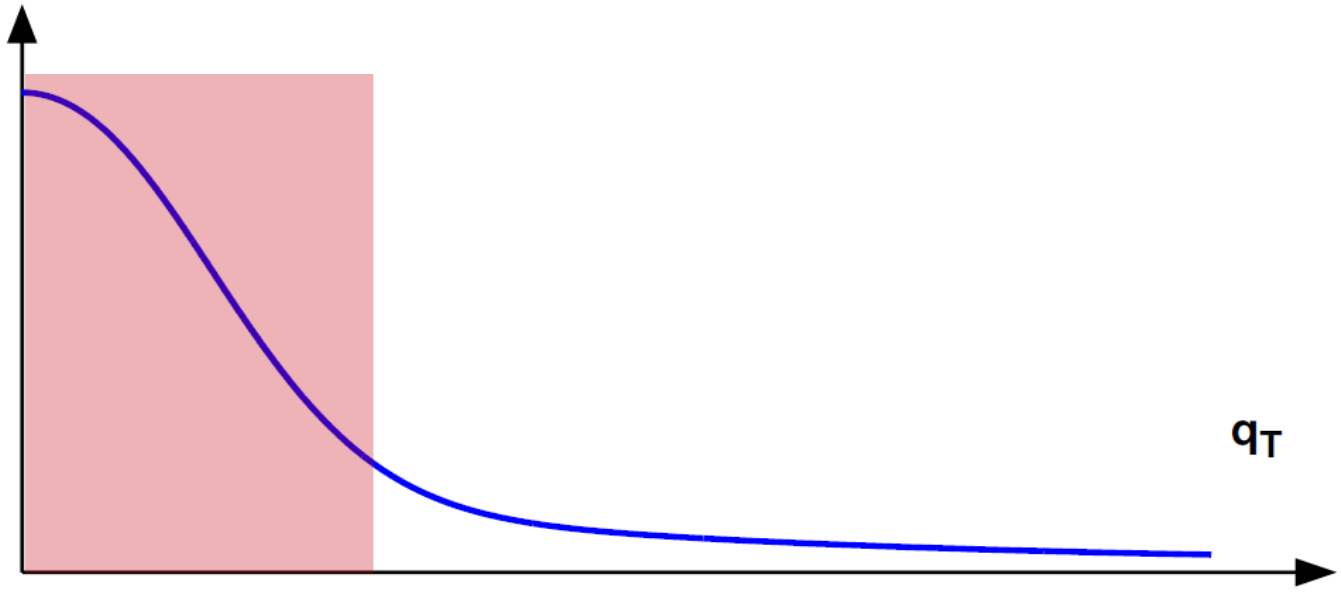

Small transverse momentum:

Harder to reproduce data as compared to simple gaussian model

W at $\mathcal{O}(\alpha_s)$ (no Y term)

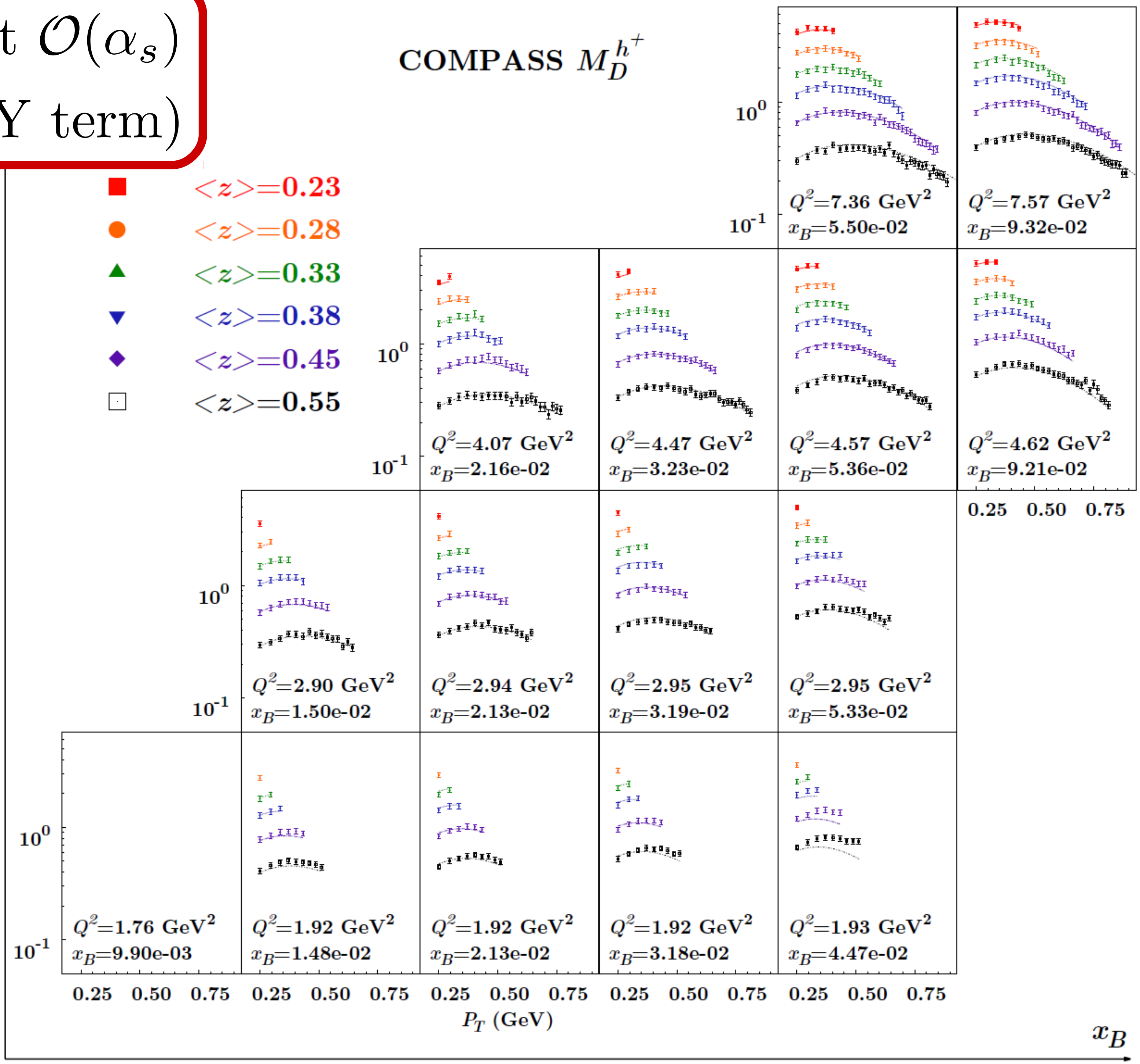

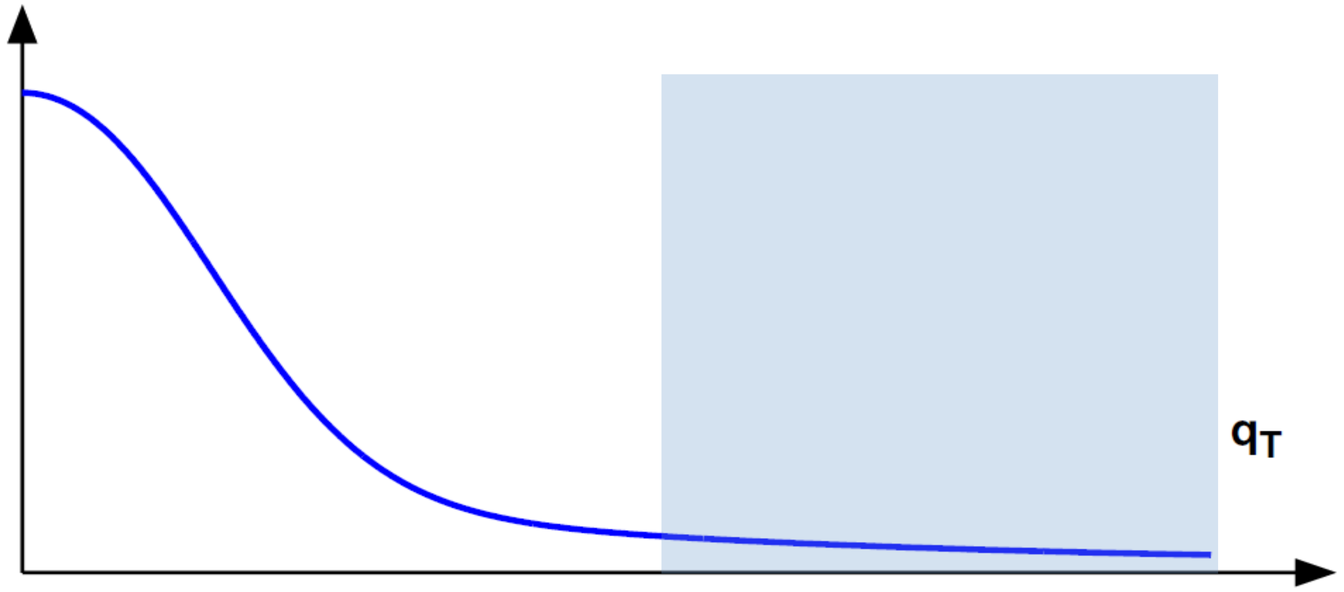

Large transverse momentum:

One would expect to be able to describe data with F. O.

At LO, F.O. is roughly an <u>order of magnitude smaller</u> than data

Try NLO ...

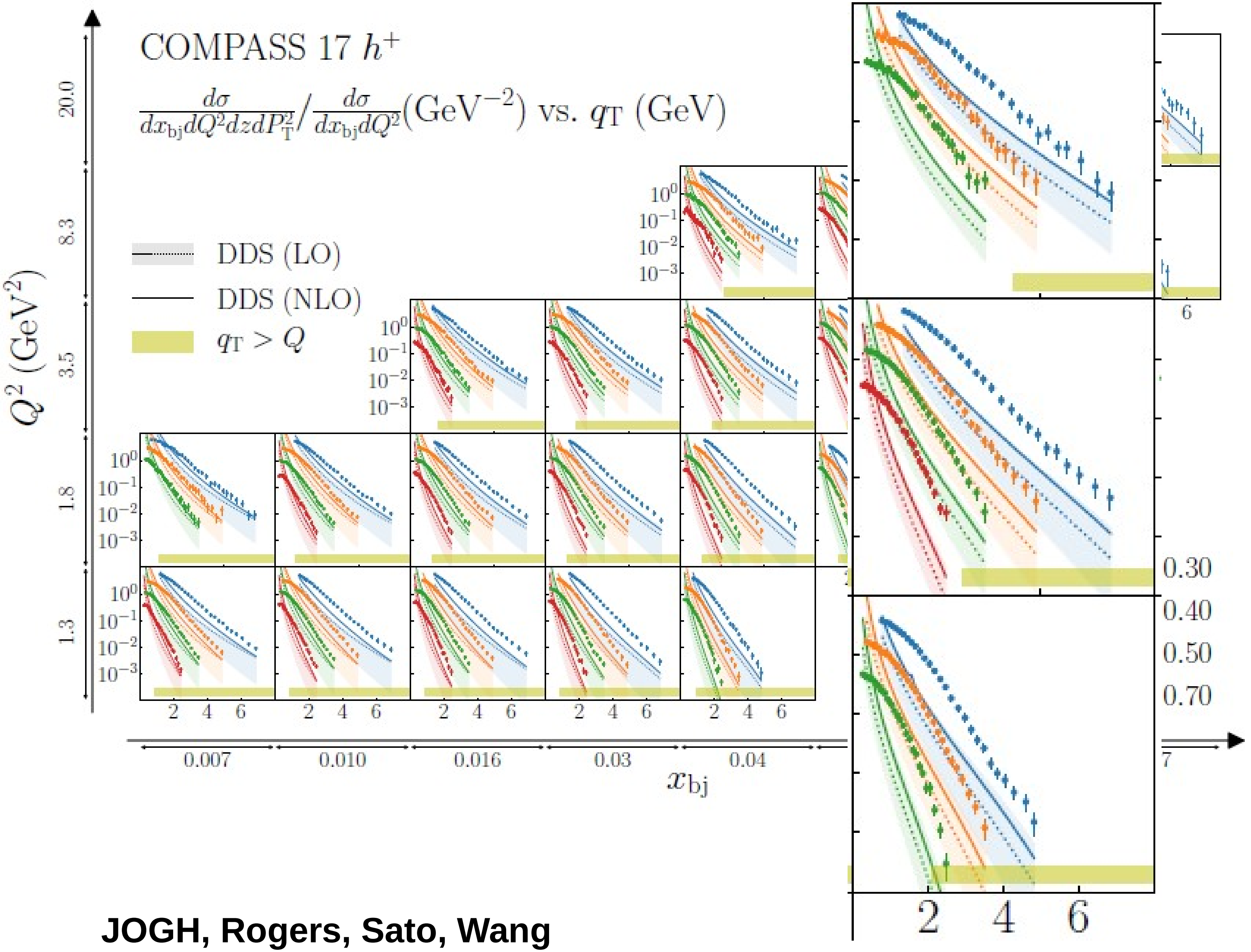

JOGH, Rogers, Sato, Wang
arXiv:1808.04396 (submitted to PRD)

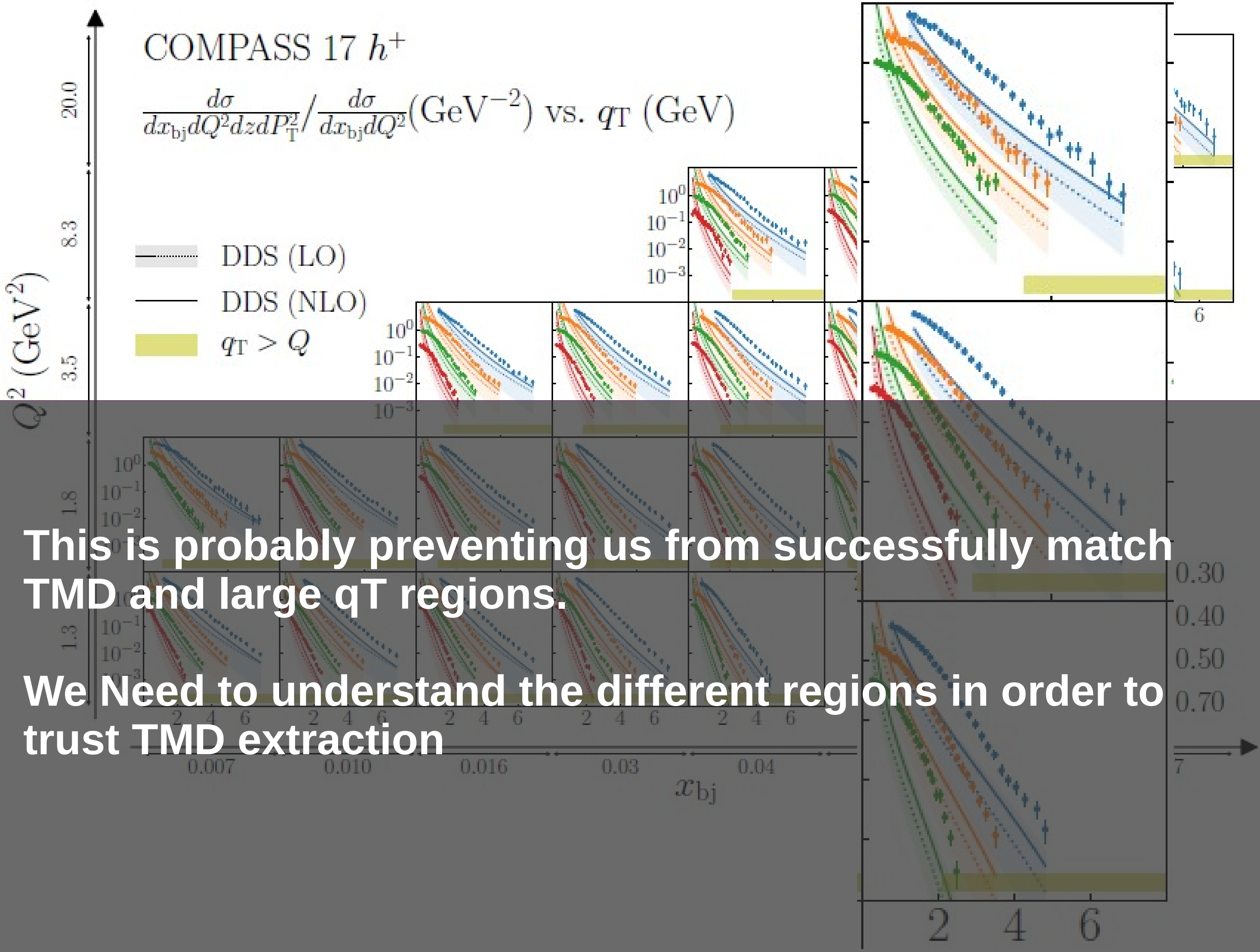

This is probably preventing us from successfully match TMD and large qT regions.

We Need to understand the different regions in order to trust TMD extraction

We need more studies on these to move to the next Stage (low energy SIDIS and Drell-Yan).

$$F_{UT}^{\sin(\phi_h-\phi_S)} \sim \boxed{\Delta^N f_{q/p^\uparrow}(x,k_\perp,Q^2)} \otimes \boxed{D(z,p_\perp,Q^2)}$$

$$F_{UU} \sim \boxed{F(x,k_\perp,Q^2) \otimes D(z,p_\perp,Q^2)}$$

And come back to this

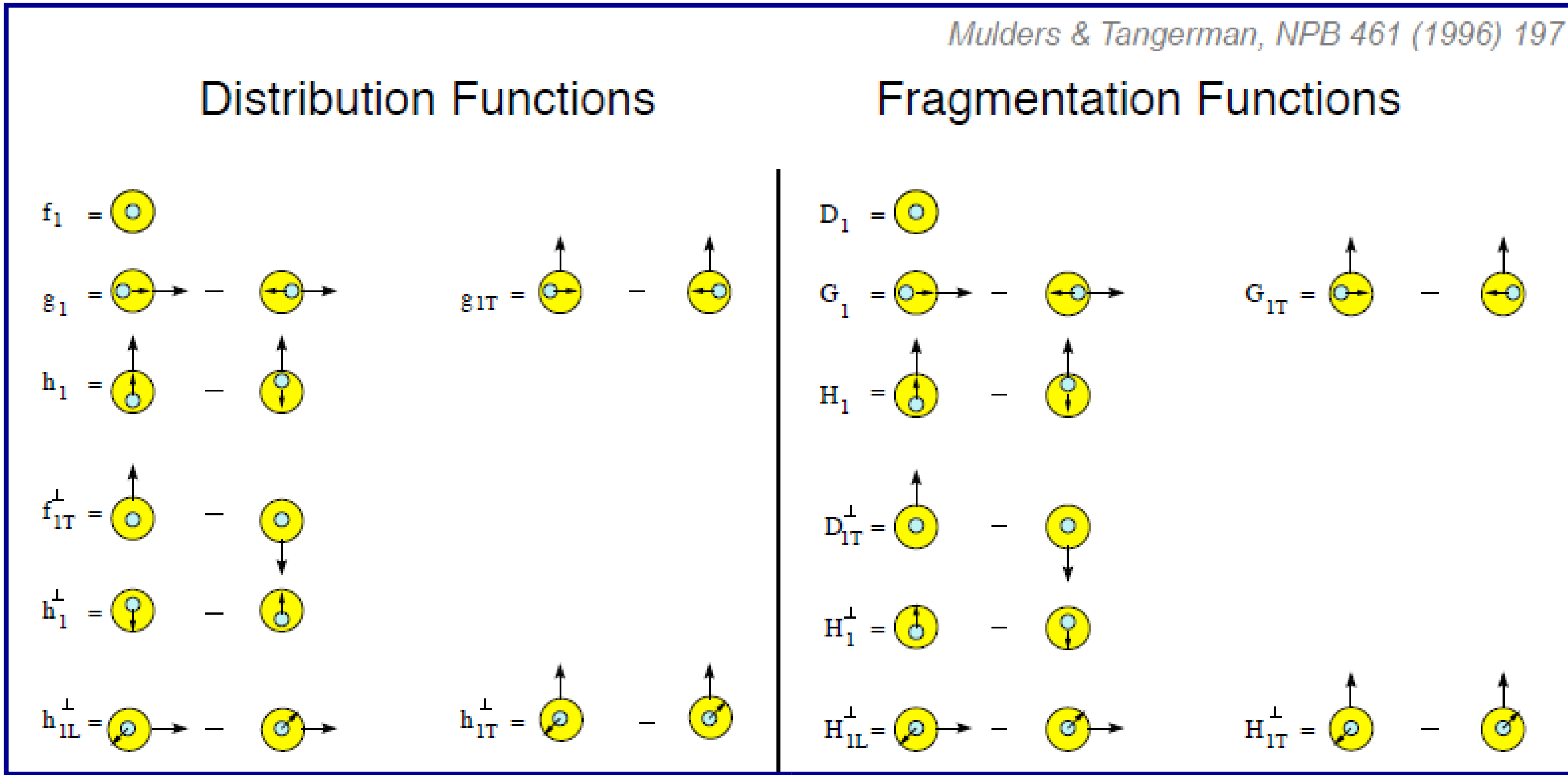
Mulders & Tangerman, NPB 461 (1996) 197
Distribution Functions
Fragmentation Functions
$f_1 =$
$g_1 =$
$h_1 =$
$g_{1T} =$
$f_{1T}^{\perp} =$
$h_1^{\perp} =$
$h_{1L}^{\perp} =$
$h_{1T}^{\perp} =$
$D_1 =$
$G_1 =$
$H_1 =$
$G_{1T} =$
$D_{1T}^{\perp} =$
$H_1^{\perp} =$
$H_{1L}^{\perp} =$
$H_{1T}^{\perp} =$

And this!

Conclusions.

New analysis on Sivers asymmetries was presented.

Sivers function in u/d channels compatible with previous extractions

Need more data to constraint d (sea)

TMD evolution effects are hard to observe in the data

Scale dependence due to Twist-3 related may be visible from data

Need to continue improving on unpolarized function (low energies):

- Understand large qT behavior
- Successful matching to TMD region

Good progress, hopefully more studies will come in the near future that allow to move from exploratory to high precision (low energy)

Thank you.

Back up

$$f_{q/p}(x,k_\perp) = f_{q/p}(x)\,\frac{e^{-k_\perp^2/\langle k_\perp^2\rangle}}{\pi\langle k_\perp^2\rangle}$$

$$D_{h/q}(z,p_\perp) = D_{h/q}(z)\,\frac{e^{-p_\perp^2/\langle p_\perp^2\rangle}}{\pi\langle p_\perp^2\rangle}\,.$$

Different widths

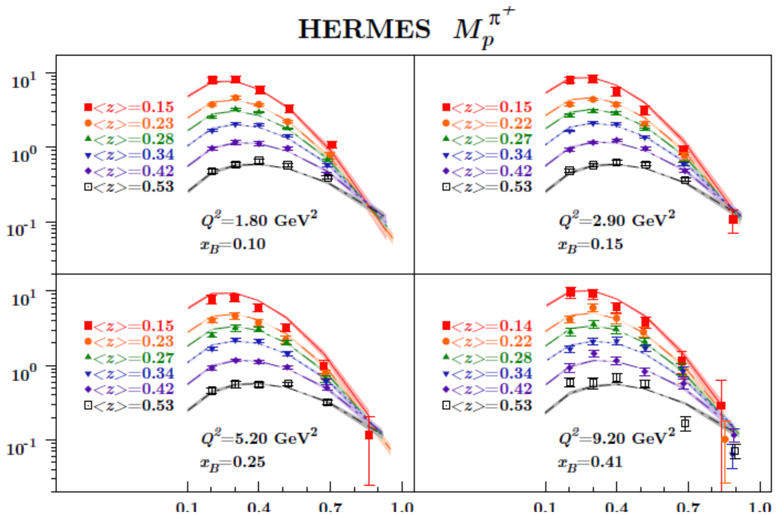

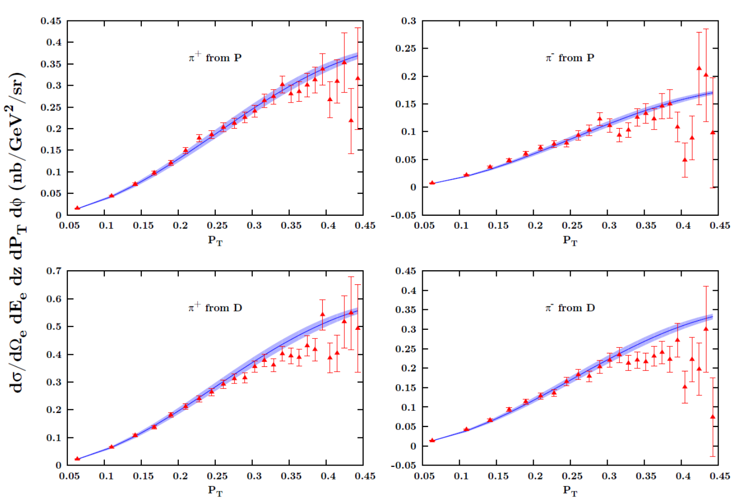

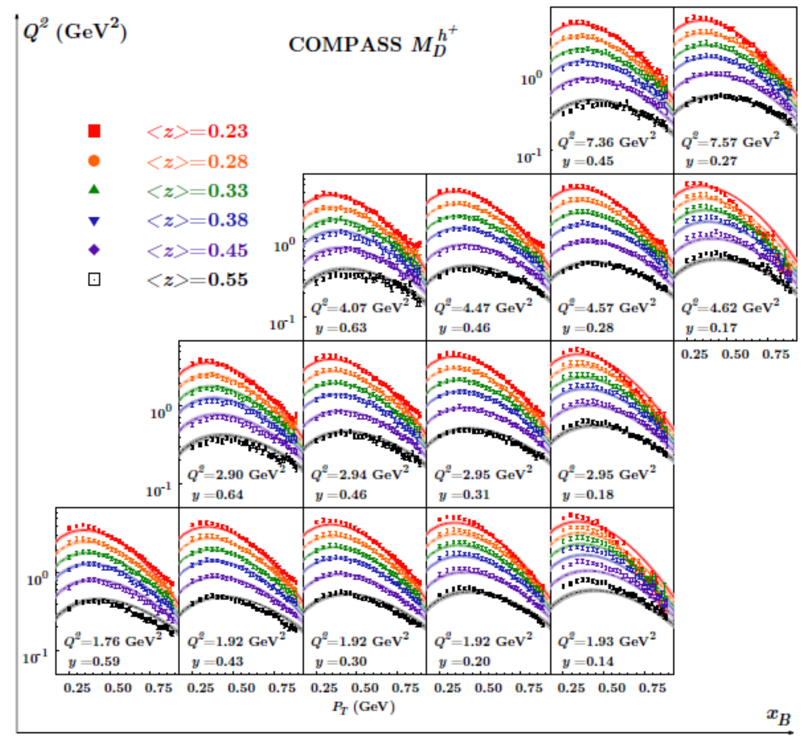

JHEP 1404 (2014) 005 Anselmino, Boglione, Melis, JOGH, Prokudin

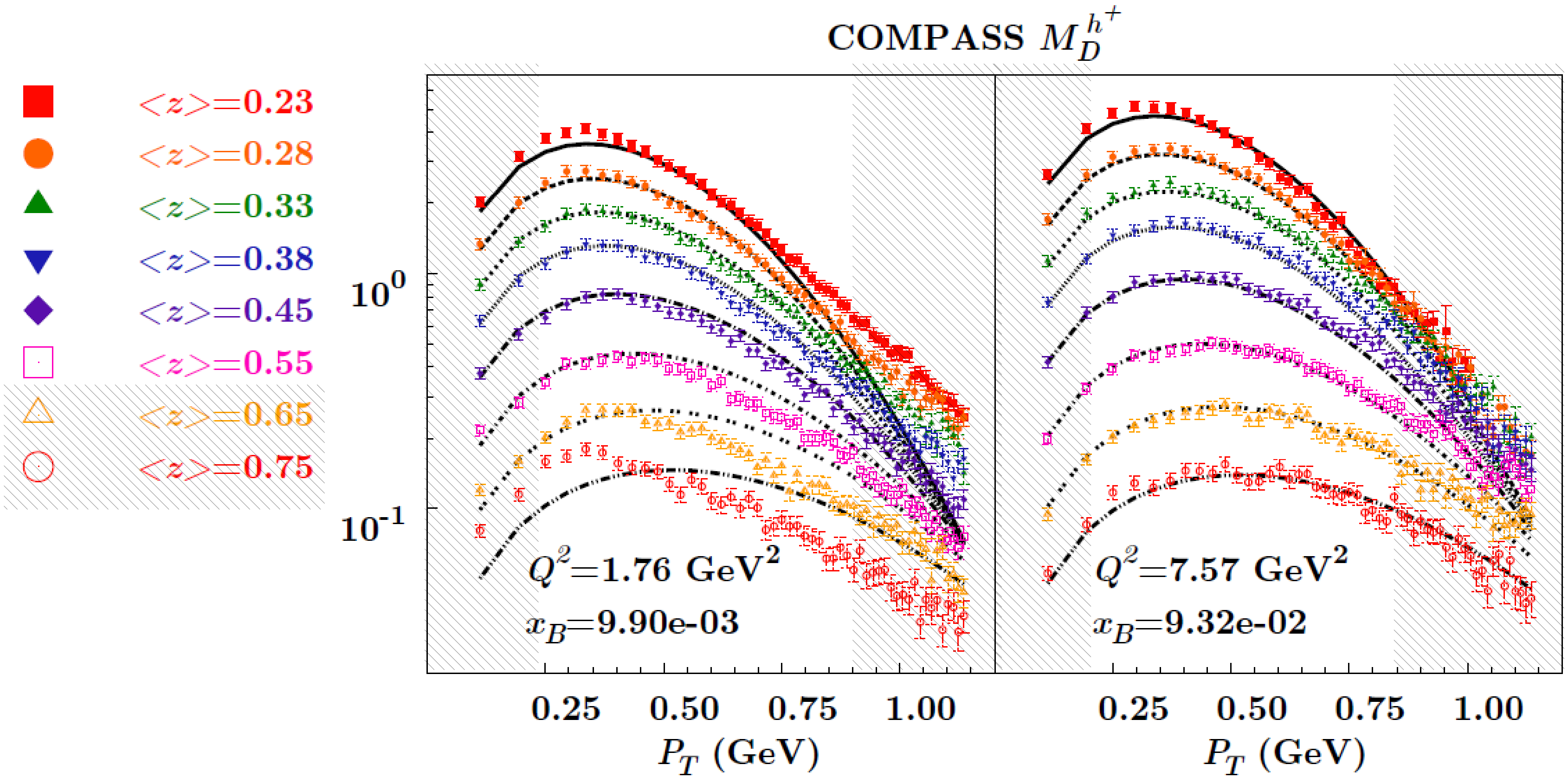

COMPASS $M_D^{h^+}$
$<z>$=0.23
$<z>$=0.28
$<z>$=0.33
$<z>$=0.38
$<z>$=0.45
$<z>$=0.55
$<z>$=0.65
$<z>$=0.75
10^0
10^{-1}
Q^2=1.76 GeV^2
x_B=9.90e-03
Q^2=7.57 GeV^2
x_B=9.32e-02
0.25
0.50
0.75
1.00
P_T (GeV)

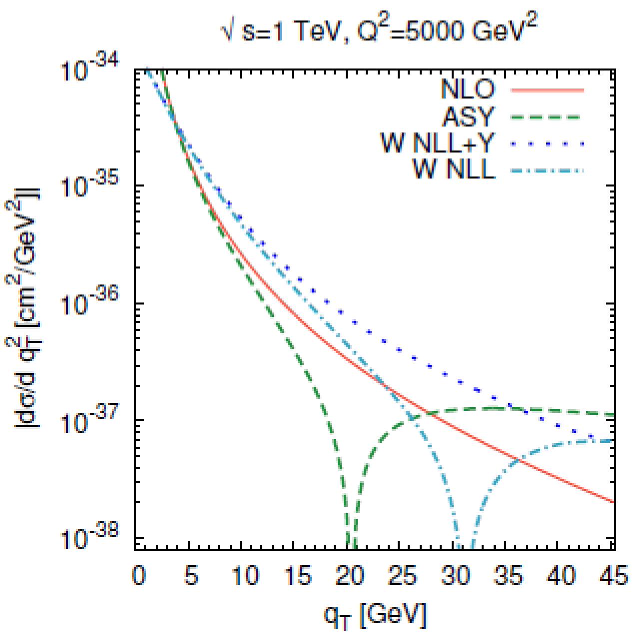

Matching is crucial, cannot afford to miss any constraint.

Historical note

ANL-HEP-CP-87-45
April 30, 1987

$$y_h = \frac{1}{2} \ln \left[\frac{E_h + p_{h,L}}{E_h - p_{h,L}} \right],$$

where $E_h, p_{h,L}$ are the energy and longitudinal component of momentum of hadron h. (Longitudinal is defined by the direction of the momentum $\mathbf{q}$.) The full range of y_h allowed kinematically is $Y = \ln W_X^2 = \ln(Q^2(1-x)/x)$; W_X is the invariant mass of the system X in the fully inclusive $eA \to e'X$.

It has been established[13] experimentally that the typical hadronic correlation length in rapidity is $\Delta y_h \simeq 2$. Therefore, if the dynamics of quark fragmentation is to be studied independently of "contamination" from target fragmentation, it is necessary that $Y \gtrsim 4$, or, equivalently, that

$$W_X = \left[\frac{Q^2(1-x)}{x} \right]^{1/2} \gtrsim 7.4\mathrm{GeV}. \tag{17}$$

Historical note

ANL-HEP-CP-87-45
April 30, 1987

$$y_h = \frac{1}{2} \ln \left[\frac{E_h + p_{h,L}}{E_h - p_{h,L}} \right],$$

where $E_h, p_{h,L}$ are the energy and longitudinal component of momentum of hadron h. (Longitudinal is defined by the direction of the momentum **q**.) The full range of y_h allowed kinematically is $Y = \ln W_X^2 = \ln(Q^2(1-x)/x)$; W_X is the invariant mass of the system X in the fully inclusive $eA \to e'X$.

It has been established[13] experimentally that the typical hadronic correlation length in rapidity is $\Delta y_h \simeq 2$. Therefore, if the dynamics of quark fragmentation is to be studied independently of "contamination" from target fragmentation, it is necessary that $Y \gtrsim 4$, or, equivalently, that

$$W_X = \left[\frac{Q^2(1-x)}{x} \right]^{1/2} \gtrsim 7.4\text{GeV}. \tag{17}$$

If the inequality Eq. (17) is satisfied, it should be possible to measure fragmentation functions $D(z, Q^2)$ over essentially the full range of z, $0 < z < 1$. Somewhat smaller values of W_X may be adequate if attention is restricted to the large z region. As Y is increased

More recently

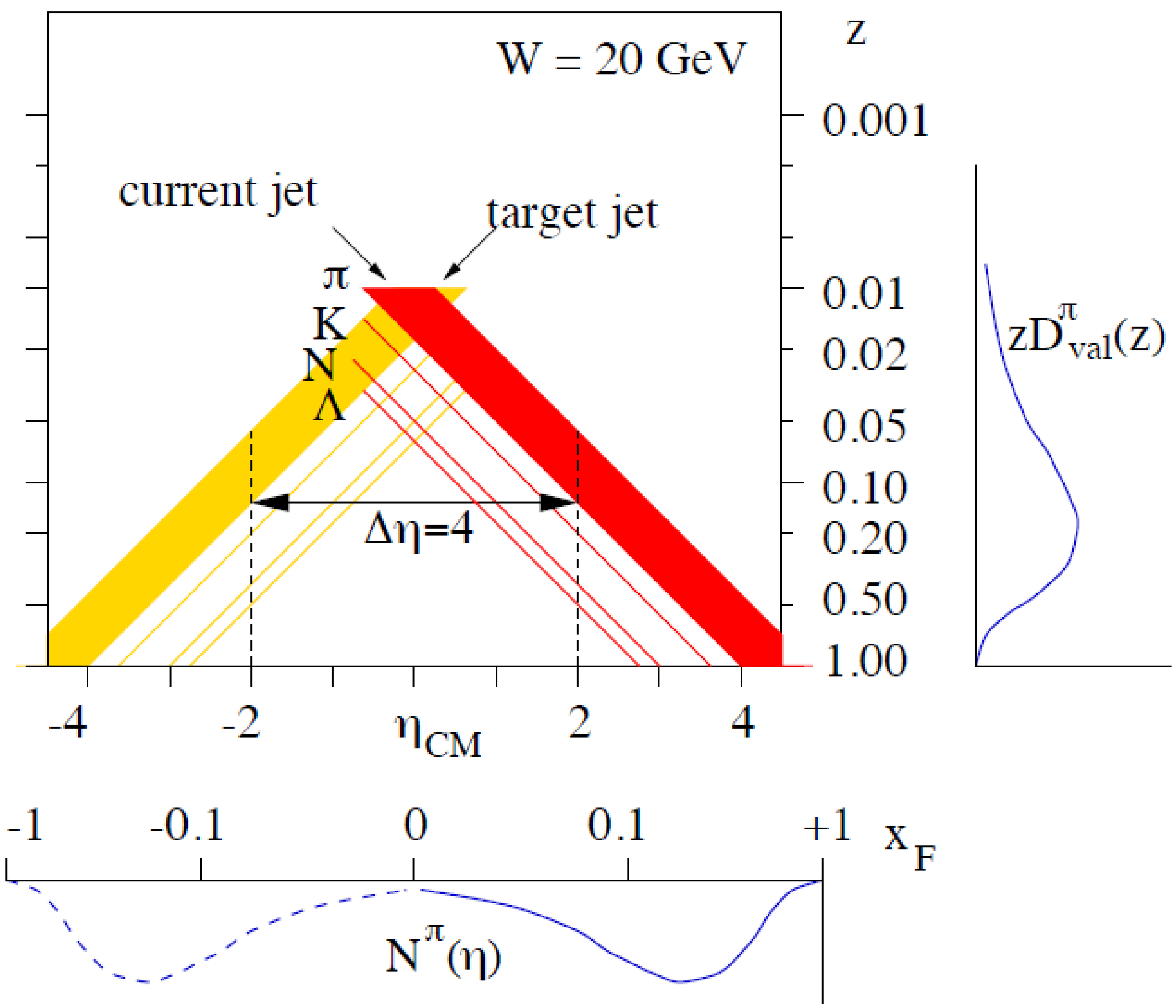

FIGURE 3. Relation between $z-values$ in fragmentation and CM rapidity for $W = 20$ GeV.

P.J. Mulders AIP Conf.Proc. 588 (2001) 75-88

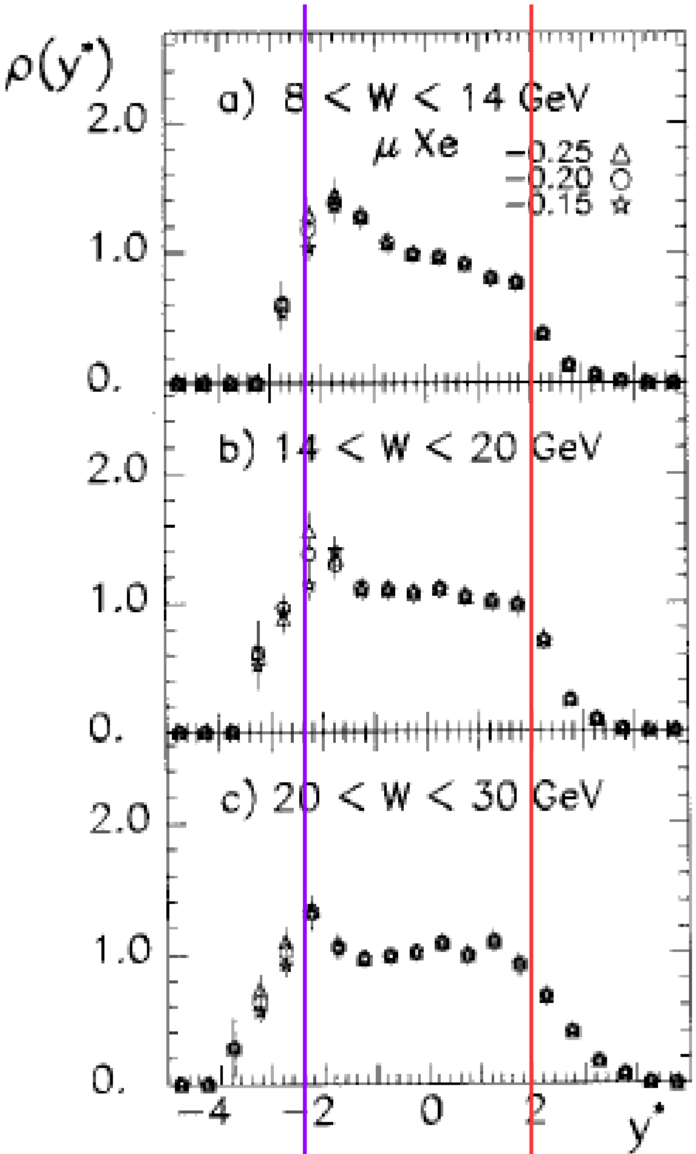

A real-life example

Rapidity distributions can be extremely useful

Z. Phys. C 61, 179–198 (1994)

E665 Collaboration

Fig. 23a–c. Normalized cms-rapidity distribution of positive hadrons in μXe scattering, in three bins of W, for three variants of the particle identification procedure (see Sect. 3.1): assignment of the proton mass if $x_F\ (m_\pi)$ is < -0.15 (stars), or if $x_F\ (m_\pi)$ is < -0.20 (circles), or if $x_F\ (m_\pi)$ is < -0.25 (triangles)